TU Delft

Delft University of Technology

Document Version
Final published version

Licence
Dutch Copyright Act (Article 25fa)

Citation (APA)
Zhao, X., Pertijs, M., & Manzaneque, T. (2026). A High-Performance PMUT Array Based on Bilayer Lithium Niobate. In *Proceedings of the 2026 IEEE 39th International Conference on Micro Electro Mechanical Systems (MEMS)* (pp. 1217-1220). IEEE. https://doi.org/10.1109/MEMS64181.2026.11419263

Important note
To cite this publication, please use the final published version (if applicable).
Please check the document version above.

Copyright
In case the licence states “Dutch Copyright Act (Article 25fa)”, this publication was made available Green Open Access via the TU Delft Institutional Repository pursuant to Dutch Copyright Act (Article 25fa, the Taverne amendment). This provision does not affect copyright ownership.
Unless copyright is transferred by contract or statute, it remains with the copyright holder.

Sharing and reuse
Other than for strictly personal use, it is not permitted to download, forward or distribute the text or part of it, without the consent of the author(s) and/or copyright holder(s), unless the work is under an open content license such as Creative Commons.

Takedown policy
Please contact us and provide details if you believe this document breaches copyrights.
We will remove access to the work immediately and investigate your claim.

This work is downloaded from Delft University of Technology.

A HIGH-PERFORMANCE PMUT ARRAY BASED ON BILAYER LITHIUM NIOBATE

Xiaoxi Zhao, Michiel Pertijs, and Tomás Manzaneque
Electronic Instrumentation Laboratory (EI), Department of Microelectronics,
Delft University of Technology, The Netherlands

ABSTRACT

This work demonstrates a linear PMUT array based on a bilayer X-cut lithium niobate ($LiNbO_3$) structure. Leveraging $LiNbO_3$'s high piezoelectric coefficients and the bilayer's ability to harness the sign-changing in-plain strain associated to plate bending, the device achieves high transmit sensitivity (0.48 kPa/V at 10 mm), high current receive sensitivity (0.56 nA/Pa), high voltage receive sensitivity (2.26 μV/Pa), and a low noise-equivalent pressure (0.18 mPa/√Hz). The array operates at 1 MHz with a fractional bandwidth of 82.5% (-6dB) and has an active area of 0.173 mm^2. Figures of merit (FoMs) that capture the sensitivity–bandwidth–area trade-offs are reported and benchmarked with other PMUT technologies. The results position bilayer $LiNbO_3$ as a promising route to compact, high-performance ultrasonic transducers.

KEYWORDS

Piezoelectric micromachined ultrasonic transducers (PMUT), lithium niobate ($LiNbO_3$), lateral-field excitation (LFE), mechanical resonator, bending mode.

INTRODUCTION

Among micromachined ultrasonic transducers (MUTs), piezoelectric MUTs (PMUTs) offer the advantages of not requiring DC bias, inherently linear response and high deflection dynamic ranges, while retaining on-chip integration capability. These features are especially appealing for emerging applications such as wearable ultrasonics and harmonic imaging. Despite these advantages, state-of-the-art PMUTs still face limited transmit (TX) and receive (RX) sensitivities, which are dominated by the properties of the piezoelectric materials employed. Prior research shows that scandium-doped aluminum nitride (ScAlN) approximately doubles the piezoelectric coefficient of AlN and improves overall PMUT performance [1], [2], [3]. Nevertheless, ScAlN PMUTs still exhibit limited transduction. More recently, potassium sodium niobate (KNN) based PMUTs have shown strong transmit sensitivity [4], [5], but fabricating high-quality thin films remains a considerable challenge. In contrast, recent studies have demonstrate lithium niobate ($LiNbO_3$) as a well-balanced PMUT platform owing to its low dielectric loss and high piezoelectric response at specific crystallographic orientations [6], [7], [8]. Our previous work [9] introduced the first bilayer $LiNbO_3$ PMUT, and preliminary displacement measurements indicated strong potential for high acoustic performance.

Building on that foundation, this work demonstrates a 12×1 linear array based on bilayer X-cut $LiNbO_3$ structure, and provides comprehensive characterization, including acoustic transmission and reception sensitivities. In addition, we also introduce figures of merit (FoMs) that enable fair cross-platform comparison by capturing trade-offs among sensitivity, bandwidth, and active area.

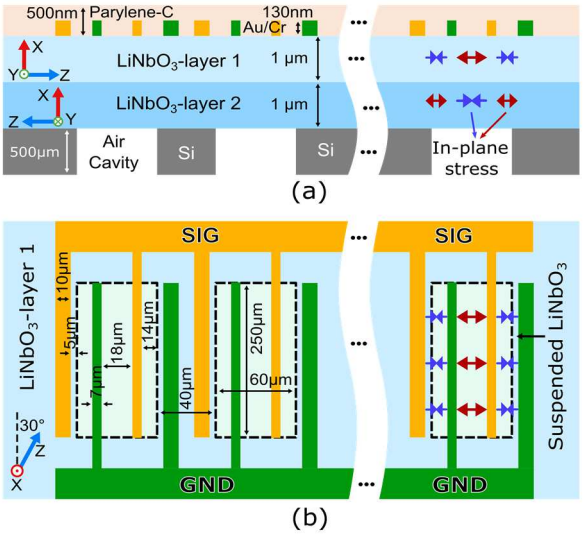


Figure 1: Schematic of the bilayer $LiNbO_3$ PMUT array: (a) cross-sectional and (b) top view. The key dimensions are labeled.

DESIGN AND FABRICATION

Bilayer working concept and PMUT array design

Fig. 1(a) shows the cross-section of the proposed PMUT array, which employs a bilayer $LiNbO_3$ structure comprising two X-cut $LiNbO_3$ films rotated 180° in-plane relative to each other. The in-plane rotation yields opposite poling directions (Z-axis), so that, under the same applied lateral electric field excitation, the two layers generate opposite piezoelectric stresses that sum to increase the bending moment, thereby enhancing electromechanical transduction relative to conventional devices with a single active layer [9]. With equal layer thicknesses, the neutral axis of the composite plate lies at the bilayer interface, fully leveraging the generated in-plane stress. For measurements in water, a 500-nm Parylene-C coating is used as an electrical insulating layer.

As shown in the top view [Fig. 1(b)], the interdigitated electrodes are rotated 30° in-plane with respect to the Z-axis to maximize the electromechanical transduction. Each PMUT element has a rectangular suspended area of 60×250 $μm^2$ with a center-to-center pitch of 100 μm. The length is designed to be much longer than the width to reduce mode distortion and maximize transduction [10]. Electrode dimensions and spacings are indicated in Fig. 1(b).

Fabrication

As shown in Fig. 2, PMUTs were fabricated on a bilayer $LiNbO_3$-on-Si stack (NGK Insulators, Ltd.). First, top

2026 IEEE 39th International Conference on Micro Electro Mechanical Systems (MEMS) | 979-8-3315-7251-8/26/$31.00 ©2026 IEEE | DOI: 10.1109/MEMS64181.2026.11419263

Authorized licensed use limited to: TU Delft Library. Downloaded on March 12,2026 at 09:55:01 UTC from IEEE Xplore. Restrictions apply.

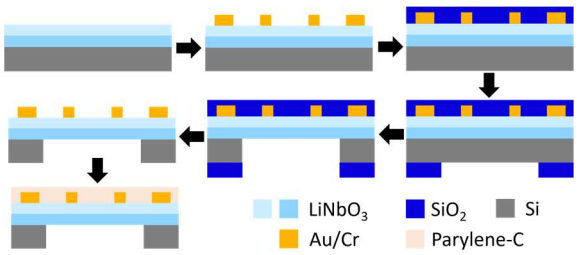


Figure 2: Double-sided fabrication process. flow.

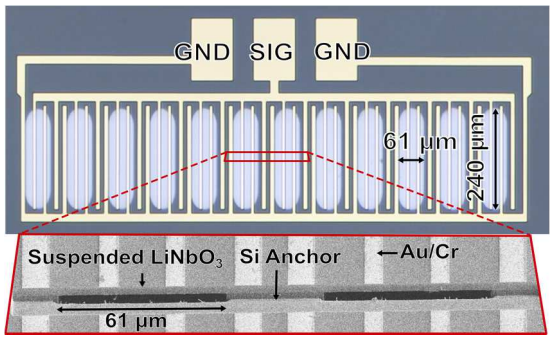


Figure 3: Fabricated devices. Top: optical image of the 12×1 array. Bottom: FIB-SEM image of two PMUT elements (52° tilt).

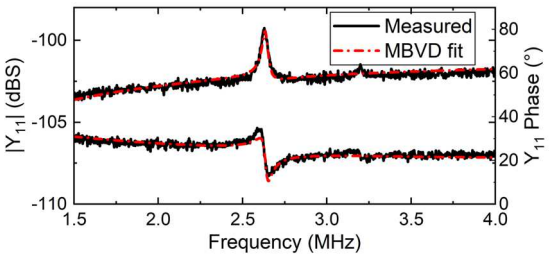
electrodes (120-nm Au/10-nm Cr) were deposited and patterned. The electrodes were then protected with a 3-µm SiO_2 layer deposited by inductively coupled plasma enhanced chemical vapor deposition (ICPECVD). After flipping the sample, a 9-µm SiO_2 hard mask was deposited on the Si backside to define the cavity etch window. Following backside alignment to the predefined electrode patten, the SiO_2 hard mask was etched via reactive ion etching (RIE). The Si substrate was subsequently etched from the bottom using the Bosch process to release the $LiNbO_3$ membranes. Finally, a 500-nm Parylene-C film was conformally deposited by chemical vapor deposition (CVD) as insulating layer for operation in water.

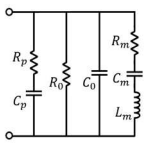
A fabricated 12×1 array is shown in Fig. 3 with the key dimensions labeled. The fabricated array show dimensions in good agreement with the design values, and exhibits a slight lateral misalignment of around 2 µm. A cross-section cut of the suspended $LiNbO_3$ was obtained using focused-ion-beam (FIB). The resulting scanning electron microscopy (SEM) image confirms uniform $LiNbO_3$ thickness across the suspended region.

EXPERIMENTAL RESULTS

Electrical characterization in air

A single-element PMUT, fabricated on the same process as the array, was used to evaluate the electromechanical coupling while eliminating the inter-element parasitics. The electrical admittance Y_{11} was measured using an impedance analyzer (Keysight E4990A). As shown in Fig. 4, the measured Y_{11} was fitted using a modified Butterworth-Van Dyke (MBVD) model, in which R_p and C_p capture the substrate-induced parasitics. Despite significant parasitic effects, the extracted electromechanical coupling factor after de-embedding the admittance of connection pads is $k_t^2 = 6.6\%$ (defined as $k_t^2 = \pi^2/8 \cdot C_m/C_0$), which is more than





Symbol	value	Symbol	value
R_m	325 kΩ	R_0	410 kΩ
C_m	2.8 fF	C_p	0.7 pF
L_m	1.3 H	R_p	174 kΩ
C_0	52 fF	k_t^2	6.6%

Figure 4: Measured admittance Y_{11} of a single-element PMUT and MBVD fit. The MBVD model and extracted parameters are shown below.

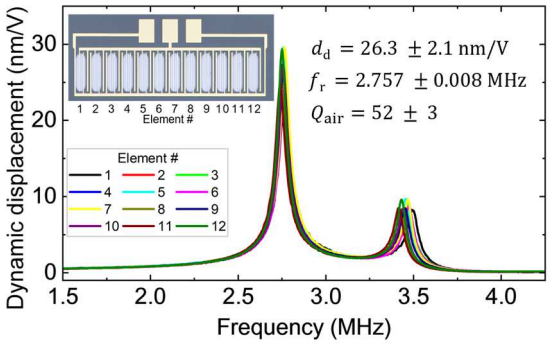


Figure 5: LDV characterization (in air) of a 12×1 array.

three times that of a representative ScAlN-PMUTs [1].

Mechanical characterization in air

The described 12×1 array was wire-bonded to a printed circuit board (PCB) and measured in air using a laser Doppler vibrometer (LDV; Polytec MSA400). As shown in Fig. 5, all elements exhibit closely matched resonant frequencies ($f_r = 2.757 \pm 0.008$ MHz), quality factors ($Q_{air} = 52 \pm 3$), and dynamic displacement sensitivities at resonance ($d_d = 26.3 \pm 2.1$ nm/V). Correspondingly, the static displacement sensitivity is given by $d_s = d_d/Q_{air} = 0.51 \pm 0.02$ nm/V. This d_s is nearly 3 times higher than the ScAlN-based PMUTs [1].

Acoustic characterization in water

Acoustic transmit (TX) and receive (RX) sensitivities were evaluated in water using the setup shown in Fig. 6. For TX, the PMUT array was driven by a 10 V peak-to-peak sine wave and the radiated sound pressure was measured by a calibrated hydrophone. To match the calibration condition, the hydrophone output was terminated with a 50 Ω adapter at the oscilloscope input. First, a 30-cycle burst at 1.0 MHz was applied to the PMUT while the transmitted sound wave was recorded by the hydrophone. The received signal shows a 32.5 µs delay, consistent with the distance $r = 50$ mm from the PMUT surface to the hydrophone [Fig. 7(a)]. An exponential fit to the ring-down envelope of the hydrophone recorded waveform yields a quality factor of $Q_{water} \approx 2.1$,

Authorized licensed use limited to: TU Delft Library. Downloaded on March 12,2026 at 09:55:01 UTC from IEEE Xplore. Restrictions apply.

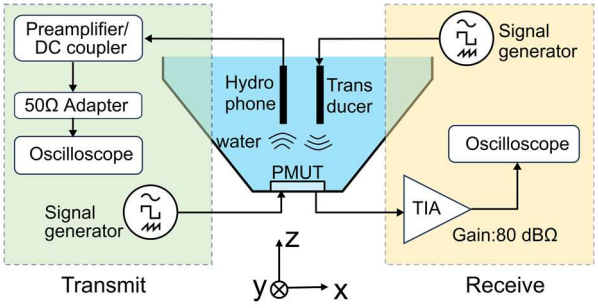


Figure 6: Schematic of the acoustic measurement setup.

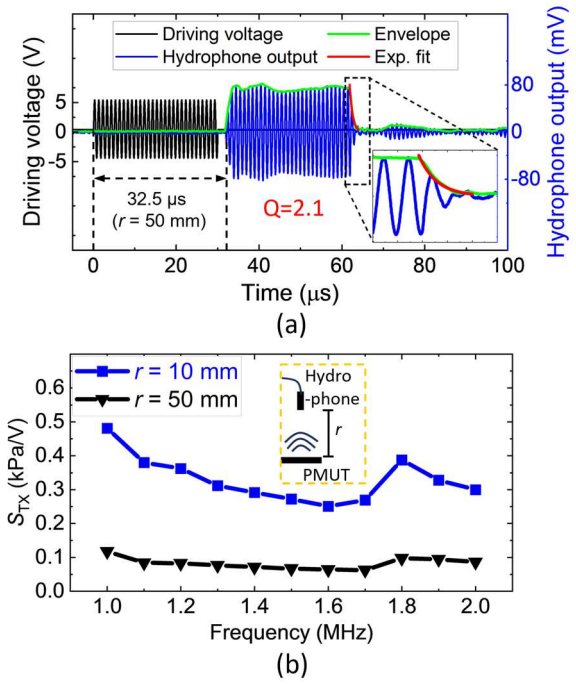


Figure 7: Transmit (TX) characterization: (a) time response under excitation of a 30-cycle burst at 1.0 MHz. (b) transmit sensitivity (S_{TX}) versus frequency.

corresponding to ~47.6% (−3 dB) and ~82.5% (−6 dB) fractional bandwidth (FBW). Next, the transmit sensitivity (S_{TX}) was measured under continuous-wave excitation at $r = 50$ mm and $r = 10$ mm [Fig 7(b)]. The frequency response exhibits a broad bandwidth in agreement with the burst-derived FBW. At 1.0 MHz, the transmit sensitivity is $S_{TX} = 0.48$ kPa/V at $r = 10$ mm and $S_{TX} = 0.12$ kPa/V at $r = 50$ mm, approximately following $1/r$ scaling ($S_{TX} \propto 1/r$), thus indicating the measurements are in the acoustic far field.

For RX, the incident sound wave was generated by a commercial transducer placed 50 mm away from the PMUT array. The incident sound pressure was first measured with a hydrophone, revealing the pressure distribution in the x-y plane at $r = 50$ mm shown in Fig. 8(a), with an acoustic spot with a diameter of approximately 3 mm, so the centrally positioned PMUT array experiences a nearly uniform incident pressure. In water, the PMUT array's electrical impedance was measured as $Z_{\mathrm{PMUT}} = 4.03$ kΩ at 1.0 MHz. Because of its high impedance, the output signal of the PMUT array was converted to voltage using a trans-impedance amplifier

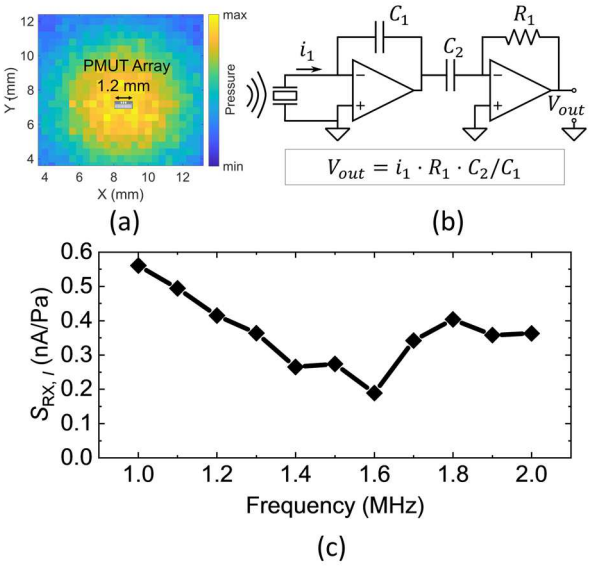


Figure 8: Receive (RX) characterization: (a) incident sound pressure pattern; (b) Schematic of TIA; (c) current sensitivity versus frequency.

(TIA). The TIA schematic is shown in Fig. 8(b); the transimpedance gain was designed to be 80 dBΩ. After de-embedding the TIA gain, the PMUT's current receive sensitivity ($S_{\mathrm{RX},I}$) is obtained and plotted in Fig. 8(c). The receiving sensitivity at 1.0 MHz is $S_{\mathrm{RX},I} = 0.56\ \mathrm{nA/Pa}$. Using the measured electrical impedance , the equivalent voltage sensitivity is given by $S_{\mathrm{RX},V} = S_{\mathrm{RX},I} \cdot Z_{\mathrm{PMUT}} = 2.26\ \mu\mathrm{V/Pa}$.

DISCUSSION

To enable a meaningful comparison of PMUTs across different material platforms, we define figures of merit (FoMs) for transmit (TX) and receive (RX) performance:

$$\mathrm{FoM_{TX}} = \frac{S_{TX} \times r}{A} \times \mathrm{FBW} \quad (1)$$

$$\mathrm{FoM_{RX}} = \mathrm{S_{RX,V}} \times \mathrm{FBW} \quad (2)$$

where S_{TX} is the transmit sensitivity, $S_{\mathrm{RX},I}$ is the current receive sensitivity, A is the PMUT active area, r is the PMUT-hydrophone spacing, and FBW is the fractional bandwidth (–6 dB). Assuming TX is measured in the far-field region, (1) compensates for the measurement distance, removing the effect from spherical spreading of acoustic power, and by the active area to reflect transmission sensitivity–area scaling. Note (2) omits the area because voltage receive sensitivity does not scale with it. Both (1) and (2) capture the inherent sensitivity–bandwidth trade-off.

Table 1 summarizes the FoMs for our PMUT array and compares it with the state-of-the-art. Compared with the ScAlN-based PMUT developed by Silterra [11], our device achieves nearly 4× higher transmit $\mathrm{FoM_{TX}}$ and 22× higher receive $\mathrm{FoM_{RX}}$. Relative to the PZT-based PMUT in [12], our device achieves approximately 4× higher $\mathrm{FoM_{TX}}$ and more than 7× higher $\mathrm{FoM_{RX}}$. Compared to the single-layer $LiNbO_3$ PMUT in [8] (RX sensitivity not reported), our bilayer $LiNbO_3$ PMUT substantially outperforms in transmit performance.

Authorized licensed use limited to: TU Delft Library. Downloaded on March 12,2026 at 09:55:01 UTC from IEEE Xplore. Restrictions apply.

Table 1. Comparison of PMUT Transmit/Receive Performance using FoMs defined in (1)-(2)

Ref.	Material	A (mm^2)	FBW (-6dB)	TX measured		TX normalized	RX measured		RX Normalized
				S_{TX} (kPa/V)	r (mm)	FoM_{TX} (kPa/V/mm)	$S_{RX,I}$ (nA/Pa)	$S_{RX,V}$ (μV/Pa)	FoM_{RX} (μV/Pa)
This work	$LiNbO_3$	0.173	82.5%	0.48	10.0	22.89	0.56	2.26	1.87
[11]	ScAlN	0.185	50.0%	1.31	1.5	5.31	N/A	0.17	0.085
[12]	PZT	3.610	30%	6.86	10.0	5.70	N/A	0.8	0.24
[8]	$LiNbO_3$	0.432	70.1%	0.94	1.2	1.83	N/A	N/A	N/A

The noise performance of our device can be estimated using the measured Q, f_r in air and water, together with the air-loaded motional resistance of a single-element PMUT $R_{\mathrm{m,air}} = 325\ \mathrm{k\Omega}$, the water-loaded motional resistance is given by [13]

$$R_{m,water} = R_{m,air} \cdot \frac{Q_{air}}{Q_{water}} \cdot \frac{f_{r,air}}{f_{r,water}} = 22.1\ \mathrm{M\Omega}.$$

For the 12×1 array, $R_{\mathrm{m,water,array}} = 22.1/12 = 1.8\ \mathrm{M\Omega}$ and the corresponding Johnson current-noise is $i_n = \sqrt{4kT/R_{\mathrm{m,water,array}}} = 95.9\ \mathrm{fA/\sqrt{Hz}}$ ($T = 300\ \mathrm{K}$). The resulting noise-equivalent pressure (NEP) of the PMUT array gives $\mathrm{NEP} = i_n/S_{RX,I} = 0.18\ \mathrm{mPa/\sqrt{Hz}}$.

CONCLUSIONS

In this work, we demonstrate a PMUT array based on bilayer X-cut $LiNbO_3$. Thanks to $LiNbO_3$'s high piezoelectric coefficient and the bilayer structure that enhances the transduction, the device delivers high TX/RX sensitivities, wide FBW, and a low NEP, comparing favorably with alternative platforms. Despite substrate-related parasitic effects, the results establish bilayer $LiNbO_3$ as a promising route to compact, high-performance PMUT arrays.

ACKNOWLEDGEMENTS

The authors would like to thank Zu Yao Chang, Ron van Puffelen, Lukasz Pakula, Nuriel Rozsa, Henry den Bok and Tiago Costa for their lab testing support.

REFERENCES

[1] Q. Wang, Y. Lu, S. Mishin, Y. Oshmyansky, and D. A. Horsley, "Design, Fabrication, and Characterization of Scandium Aluminum Nitride-Based Piezoelectric Micromachined Ultrasonic Transducers," *J. Microelectromech. Syst.*, vol. 26, no. 5, pp. 1132–1139, Oct. 2017.

[2] J. Liu *et al.*, "Towards Unparallelled CMOS-compatible Air-coupled pMUT Performance with 30% Sc-doped AlN through an Analysis of Residual Stress Effects," in *2024 IEEE Ultrasonics, Ferroelectrics, and Frequency Control Joint Symposium (UFFC-JS)*, Sep. 2024, pp. 1–4.

[3] C. B. Karuthedath, A. T. Sebastian, P. Helistö, T. Sillanpää, and A. Kärkkäinen, "Development of ScAlN PMUTs for Medical Applications," *J. Microelectromech. Syst.*, vol. 32, no. 5, pp. 505–512, Oct. 2023.

[4] L. Zhao, C. Yang, X. Zhang, Z. You, and Y. Lu, "Design, Fabrication, and Characterization of High-Performance PMUT Arrays Based on Potassium Sodium Niobate," *Journal of Microelectromechanical Systems*, vol. 33, no. 4, pp. 438–445, Aug. 2024.

[5] F. Xia *et al.*, "High sound pressure piezoelectric micromachined ultrasonic transducers using sputtered potassium sodium niobate," *Microsyst Nanoeng*, vol. 10, no. 1, p. 205, Dec. 2024.

[6] R. Lu, M. Breen, A. E. Hassanien, Y. Yang, and S. Gong, "A Piezoelectric Micromachined Ultrasonic Transducer Using Thin-Film Lithium Niobate," *J. Microelectromech. Syst.*, vol. 29, no. 6, pp. 1412–1414, Dec. 2020.

[7] X. Meng *et al.*, "Design of High-Sensitivity Piezoelectric Micromachined Ultrasonic Transducer Based on Single-Crystal Lithium Niobate Thin Films," *IEEE Transactions on Electron Devices*, pp. 1–8, 2025.

[8] X. Meng *et al.*, "A High Bandwidth PMUT Based on X-Cut Single-Crystal Lithium Niobate for Underwater Communication," *IEEE Sensors Journal*, vol. 25, no. 4, pp. 6017–6024, Feb. 2025.

[9] X. Zhao, M. Pertijs, and T. Manzaneque, "Piezoelectric Micromachined Ultrasonic Transducer (PMUT) Based on Bilayer X-Cut Lithium Niobate," in *2025 23rd International Conference on Solid-State Sensors, Actuators and Microsystems (Transducers)*, Jun. 2025, pp. 530–533.

[10] X. Zhao, M. Pertijs, and T. Manzaneque, "Optimal Orientations of Lithium Niobate for Lateral-and Thickness-Field-Excitation PMUTs," in *2025 IEEE International Ultrasonics Symposium (IUS)*, Sep. 2025, pp. 1–4.

[11] E. Ledesma, A. Uranga, F. Torres, and N. Barniol, "Fully Integrated Pitch-Matched AlScN PMUT-on-CMOS Array for High- Resolution Ultrasound Images," *IEEE Sensors Journal*, vol. 24, no. 10, pp. 15954–15966, May 2024.

[12] J. Cai, Y. Wang, and T. Wu, "High-Order Piezoelectric Micromachined Ultrasonic Transducer With Piezoelectric Layer Trench for Ultrasound Imaging," *Journal of Microelectromechanical Systems*, vol. 34, no. 4, pp. 359–361, Aug. 2025.

[13] D. A. Horsley *et al.*, "Piezoelectric Micromachined Ultrasonic Transducers for Range-Finding Applications," in *2021 5th IEEE Electron Devices Technology & Manufacturing Conference (EDTM)*, Chengdu, China: IEEE, Apr. 2021, pp. 1–3.

CONTACT

*Xiaoxi Zhao, email: X.Zhao-4@tudelft.nl

Authorized licensed use limited to: TU Delft Library. Downloaded on March 12,2026 at 09:55:01 UTC from IEEE Xplore. Restrictions apply.